Fully protonated polyaniline: Hopping transport on a mesoscopic scale

R. Pelster and G. Nimtz
II. Physikalisches Institut der Universität zu Köln, Zülpicher Strasse 77, 50937 Köln, Federal Republic of Germany

B. Wessling
Zipperling Kessler & Co., Kornkamp 50, 22926 Ahrensburg, Federal Republic of Germany
(Received 25 October 1993; revised manuscript received 28 January 1994)

In order to clarify the transport mechanism in fully protonated highly conductive polyaniline, the origin and size of the electronic localization centers and barriers have to be determined. Dispersions of polyaniline in an insulating polymer have been studied by temperature-dependent broadband dielectric spectroscopy (5 Hz to 2 GHz, 100–320 K). The electronic transport in the blends and in pure polyaniline is shown to be governed by three-dimensional (3D) hopping between mesoscopic crystalline regions surrounded by amorphous polyaniline and not by intermolecular hopping or molecular scale disorder. Two independent approaches yield an average size of 8 nm for the metallic regions in polyaniline with 3D extended electron wave functions. The barrier width is estimated to be 1.6 nm. The crystalline metallic regions with an amorphous shell correspond to the primary particles which were found in morphological studies.

Protonated polyaniline (PAni-ES, the emeraldine salt form) is an intrinsically conductive polymer. Its thermal activated conductivity $\sigma = \sigma_0 \exp(-\sqrt{T_0/T})$ is attributed to electron hopping, but the origin and size of the electronic localization centers and barriers have not yet been identified. The question remains whether the conductivity is governed by centers and barriers either on molecular or on mesoscopic scales. Recently, Wang *et al.*[1] have claimed the existence of metallic crystalline regions having a mean diameter of 2 nm. However, the dc conductivity is thought to be determined by one-dimensional (1D) interchain hopping in the amorphous parts of the material. Li, Cruz, and Phillips[2] assume the metallic regions to correspond to single molecular strands between which 3D variable range hopping occurs. The existence of metallic states has been affirmed by the recent observation of a metallic behavior[3,4] of the thermoelectric power $S \propto T$, probably due to a reduced microscopic disorder.[4] The smallest units observed by morphological studies (scanning tunneling microscope,[5] membrane filtration or photon correlation spectroscopy of liquid PAni dispersions[6,7]) are primary particles having a diameter of about 10 nm. The conductivity of PAni-ES might be dominated by charge exchange between these mesoscopic units, the size of which corresponds to electronic localization lengths observed at low temperatures.[8]

The aim of the present study has been to clarify the transport mechanism, i.e., to find out whether the conductivity of polyaniline is governed by localization centers and barriers on a molecular *or* on a mesoscopic scale. As we shall show, the experimental data allows us to distinguish between the different models cited above. We have identified the basis of the hopping transport with two independent approaches. The first one allows us to calculate the size of metallic crystalline regions from their quasistatic electric polarization. The second approach yields the size of the localization centers from their charging energy, i.e., from the activation energy of the dc conductivity and the low and high frequency values of the dielectric function. We have performed broadband dielectric measurements on dispersions of fully doped polyaniline in PETG copolyester, an insulating polymer based on polyethylene terephtalate (KODAR PETG Copolyester, Eastman Chemical). Such blends provide the mechanical properties needed for technical applications, e.g., for electromagnetical shielding, and allow as well to achieve sufficiently high conductivities. The PAni-ES used was the commercially available VERSICON powder (Allied Signal Inc.; doping level $y = 0.5$, protonated with an organic acid H^+X^-). The volume fraction of crystalline material is 30% as estimated from x-ray measurements. The dc conductivity of compressed PAni pellets[3] is $\simeq 2000\ \Omega^{-1}\,m^{-1}$. Cylindrically shaped samples with metallized front faces were placed in a shielded parallel-plate condenser which was inserted into a transmission line. With a broadband calibration method[9] the complex dielectric function (DF) $\varepsilon = \varepsilon_1 - i\varepsilon_2$ can be calculated from the measured transmission coefficient of the system even at frequencies above 1 MHz. The measurements were performed with two network analyzers (5 Hz-200 MHz: HP 3577B; 200 MHz-2 GHz: HP 8510B/1000 frequency points).

Figure 1 shows the conductivity $\sigma = \varepsilon_0 \varepsilon_2 \omega$ vs frequency of different blends at room temperature. Above a critical volume filling factor $f_c = V_{\mathrm{PAni}}/V_{\mathrm{sample}} \times 100\% \simeq 8\%$ the low-frequency values equal the respective dc conductivities, i.e., there are conducting paths of PAni across the samples, whereas below f_c conductive regions of PAni are well embedded in the insulating matrix. This transition is seen more clearly in Fig. 2, where the conductivity at 5 Hz and the static dielectric constant are displayed as a function of filling factor. The results of the two regions of different inner sample topology, below and above f_c, will be discussed separately.

For $f < f_c$ a relaxation process is observed (Fig. 3), the relaxation strength of which increases with the amount

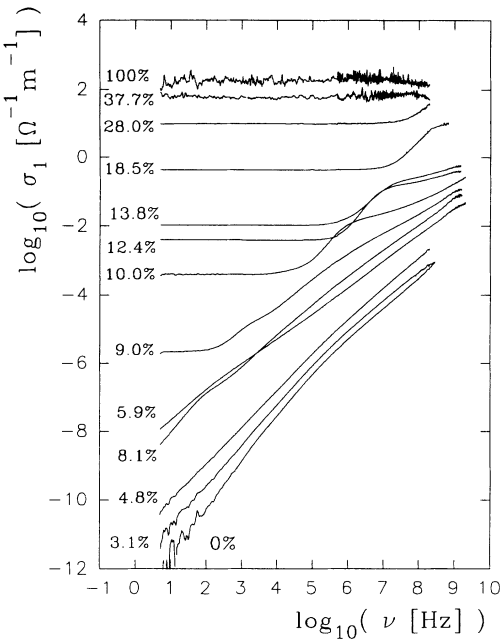

FIG. 1. Conductivity vs frequency of PAni/PETG blends with different volume filling factors in double-log plot ($T = 24\,^{\circ}\mathrm{C}$). Above $f \simeq 8\%$ the constant low-frequency values equal the dc conductivity. For $f \geq 37\%$ the measured conductivities are determined by the contact resistance of the samples. According to Subramaniam *et al.* (Ref. 3) the bulk value for pure PAni (compressed Versicon) is $\sigma \simeq 2000\ \Omega^{-1}\,\mathrm{m}^{-1}$.

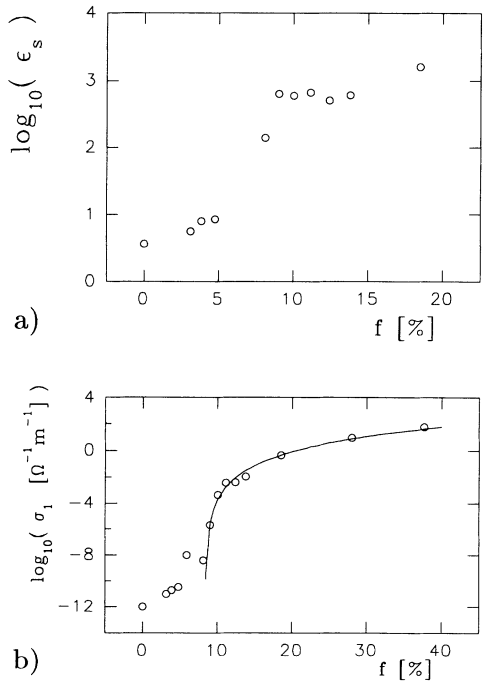

FIG. 2. (a) Extrapolated static dielectric constant and (b) conductivity at 5 Hz vs filling factor of PAni/PETG blends in semi-log plot ($T = 24\,^{\circ}\mathrm{C}$). Above $f \simeq 8\%$ the measured σ values equal the dc conductivity. —: best fit $\sigma = a(f - f_c)^{\mu}$ with $a = 8230\ \Omega^{-1}\,\mathrm{m}^{-1}$, $f_c = 0.084$ and $\mu = 4.28$. Obviously, since $\mu > 2$, there is no statistical distribution (Ref. 10) of polyaniline above f_c.

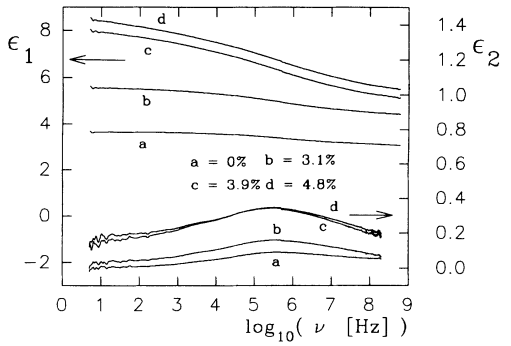

FIG. 3. Real part ε_1 (upper curves, left y axis) and imaginary part ε_2 (lower curves, right y axis) of the DF vs frequency in semi-log plot for blends below f_c ($T = 24\,^{\circ}\mathrm{C}$).

of PAni. Temperature-dependent measurements show an Arrhenius behavior $\tau = 1/(2\pi\nu_{\max}) = \tau_0 \times \exp(W/k_B T)$. Both mean activation energy $W \simeq 0.5$ eV and relaxation time $\tau_0 \simeq 10^{-15}$ s remain independent of the PAni content. By comparing the data with those of polyethylene terephtalate ($W = 0.564$ eV, $\tau_0 \simeq 5 \times 10^{-15}$ s),[11] which is similar to PETG in its chemical structure, this process was related to the β relaxation of PETG, i.e., to a dielectric relaxation of the polar carboxyl groups[12,13] (details will be published elsewhere[14]). The creation of interfaces by adding polyaniline breaks up interactions between PETG molecules and thus the number of relaxators participating in the β mechanism increases. W and τ_0 are mainly influenced by intrachain bonds and remain thus rather unchanged.

In addition, due to a mixture effect the real high-frequency value of the DF, ε_∞, increases with increasing filling factor (Figs. 3 and 4) and is rather independent of temperature. The dispersion of highly conducting PAni

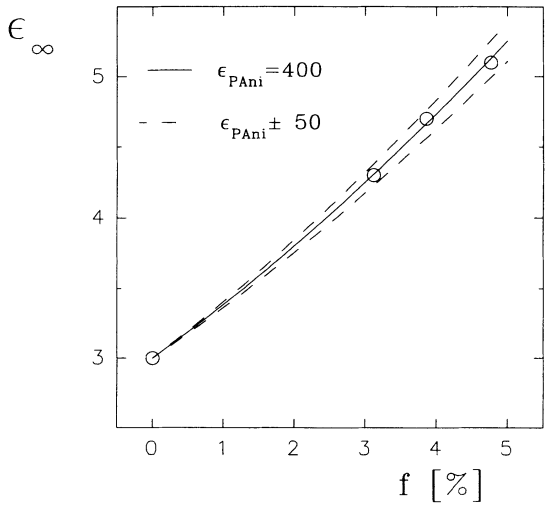

FIG. 4. High-frequency value ε_∞ vs filling factor of blends with $f < f_c$ at $24\,^{\circ}\mathrm{C}$ (extrapolated from Cole-Cole diagrams, i.e., from plots of the imaginary part of the DF vs the real part). The solid line is calculated from the Looyenga-formula with $\varepsilon_{\mathrm{PAni}} = 400$ (the uncertainty is about 20). In order to show the accuracy of the evaluation the dashed lines are calculated with $\varepsilon_{\mathrm{PAni}} = 350$ and $\varepsilon_{\mathrm{PAni}} = 450$, respectively.

in an insulating matrix below f_c yields an interfacial polarization process the relaxation frequency of which lies above the frequency range under consideration (a rough estimate can be made using the formula of Maxwell-Wagner-Sillars,[15] which yields $\nu_m \geq 4 \times 10^{12}$ Hz), i.e., there is no dissipation of energy due to free charge carriers. There are two ways for an effective medium analysis. First, to use a formula which takes into account interfacial polarization of free charge carriers and relates the bulk permittivities and conductivities of the components to those of the blend, like the Maxwell-Wagner-Sillars formula (but it is known that this formula underestimates the effective polarization in the case of a highly conductive component[16]). Second, to use a general geometry-independent mixture formula for dielectrics and to attribute a real quasistatic permittivity to the dispersed PAni, the value of which will take into account the geometrical polarization effect. Afterwards this geometry-dependent value can be analyzed. We shall use the second approach allowing us to apply the effective medium formula of Looyenga[17]

$$\varepsilon_\infty^{1/3} = f\varepsilon_{\mathrm{PAni}}^{1/3} + (1-f)\varepsilon_{\mathrm{PETG}}^{1/3}$$

which has been verified recently by 3D complex computer simulations[18,19] whereas the other formulas have been shown to fail more or less at higher permittivity ratios of the components (even at low filling factors). The formula applies also in the case of dissipative material.[19] In general the exponent depends on f but at low filling factors the value 1/3 can be used.[18,19] Thus we get for the dispersed PAni (see Fig. 4)

$$\varepsilon_{\mathrm{PAni}}(\omega\tau \ll 1) \simeq 400.$$

Undoped insulating polyaniline[1,22] exhibits a value of about $\varepsilon_c \simeq 4-10$, i.e., the quasistatic permittivity of the dispersed PAni is enhanced due to interfacial polarization. According to calculations of Cini and Ascarelli[20] this enhancement is related to the size of the conducting regions. Therefore, the total response will be governed by the larger metallic regions. For a metallic cube of side length L (standing electron waves between infinite potential walls) and for $\omega \to 0$, $\pi/L \ll k_F = (3\pi^2 n)^{1/3}$ (n: charge carrier density) holds[20]

$$\varepsilon = \varepsilon_c + Gn^{1/3}L^2$$

with $G = (2/\pi)^5 m_e e^2 (3\pi^2)^{1/3}/(\hbar^2 4\pi\varepsilon_0) = 6.09 \times 10^9$ m^{-1}. In fully protonated polyaniline every dimer contributes one charge carrier. The volume of a dimer[21] is about $11.8 \times 4.5 \times 1.6$ Å^3, the volume of the counterion X^- (Versicon: protonation with an organic acid H^+X^-) about $9.8 \times 4.5 \times 2.9$ Å^3. The average volume of a protonated dimer with counterion will thus be $V \simeq 11.8 \times 4.5 \times 4.5$ Å^3. The resulting carrier density is $n \leq n_{\max} = 1/V \simeq 4 \times 10^{27}$ m^{-3}. Accordingly the size of the metallic regions in PAni can be estimated to

$$L = \sqrt{\frac{\varepsilon_{\mathrm{PAni}} - \varepsilon_c}{G}} \frac{1}{n^{1/6}} \geq 6.3 \text{ nm}.$$

This value roughly equals the size of the so-called primary particles which were identified in morphological studies on pure PAni (also VERSICON).[5–7] A formation of agglomerates would not yield a larger value of L, presupposed there are barriers between neighboring primary particles. With $k_F \simeq 5 \times 10^9$ m^{-1} the criterion $k_F \gg \pi/L \simeq 5 \times 10^8$ m^{-1} is still fulfilled. Wang *et al.*[1] estimated $L \geq 2$ nm from measurements on orientated conductive PAni samples. They have used DF values at microwave frequencies which might be smaller than the quasistatic ones and, in addition, the polarization is weakened due to the dc conductivity of the samples. In order to find out whether these mesoscopic metallic regions dominate the transport mechanism in the blends and in pure PAni, measurements above f_c were considered.

At filling factors above f_c a process becomes visible (Fig. 5) having a relaxation time $\tau = 1/(2\pi\nu_{\max})$ which is related to the effective dc conductivity of the blends. For $f > 18.5\%$ the relaxation frequency has been shifted out of the measured range and only the high frequency-independent conductivity can be observed. With decreasing temperature or filling factor both the dc conductivity and the relaxation frequency become smaller. For nearly seven orders of magnitude holds (see Fig. 6):

$$\tau(f,T) = \frac{\zeta}{\sigma_{\mathrm{dc}}(f,T)}$$

with $\zeta \simeq 2.1 \times 10^{-10}$ (s$\,\Omega^{-1}\,$m^{-1}). The above relation is known as conduction current relaxation.[23,24] It is characteristic for a partial interfacial polarization, induced by conducting paths which are not parallel to the electric field. It has also been observed in blends of mesoscopic metal particles in insulating matrices and is a general geometric correlation between mesoscopic structure and dielectric properties.[14]

In order to interpret the transport data we consider the temperature dependence of the dc conductivity and

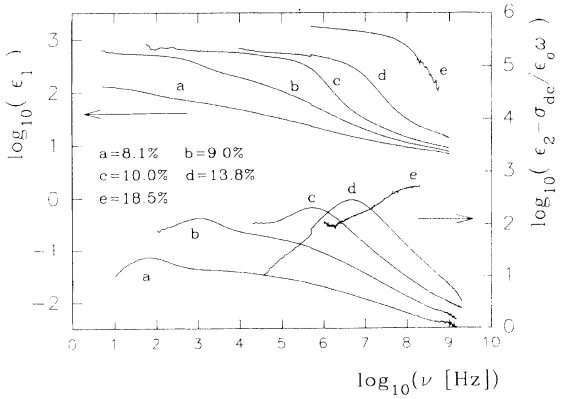

FIG. 5. Dielectric function of blends ($f \geq f_c$, 24 °C) in a double-log plot (ε_1: upper curves, left y axis; ε_2: lower curves, right y axis) The dc contribution $\sigma_{\mathrm{dc}}/\varepsilon_0\omega$ has been subtracted from the imaginary part to show more clearly the relaxation process.

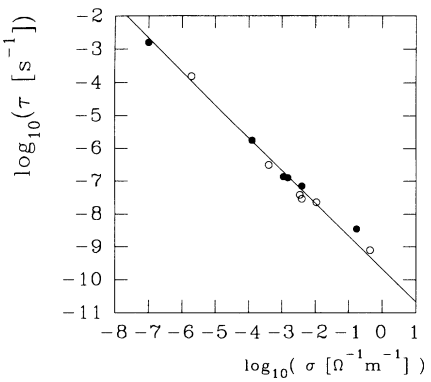

FIG. 6. Relaxation time vs dc conductivity of the process shown in Fig. 5 in double-log plot. $\tau(f,T) \propto 1/\sigma_{dc}(f,T)$ holds. Open circles: $T = 24\,^{\circ}C$. Filled circles: $T = -172\,^{\circ}C$.

the respective high and low frequency values ε_∞ and ε_s of samples with $f > f_c$. At temperatures between 200–300 K the conductivity shows an Arrhenius behavior $\sigma = \sigma_1 \exp(-W/k_BT)$ with an activation energy W of the order of magnitude of the thermal energy k_BT (see Fig. 7). At lower temperatures the Arrhenius law fails and the conductivity follows

$$\sigma = \sigma_0 \exp(-\sqrt{T_0/T}) \tag{1}$$

a relation which has also been observed in other PAni blends[3] down to temperatures of 10 K. The respective parameters for different filling factors are listed in Table I. Li, Cruz, and Phillips[2] have shown that this temperature dependence is characteristic for 3D variable range hopping with a temperature-dependent density of tunneling states $N(\varepsilon_F)$ using as an argument the linear increase of the charge carrier density with temperature. Equation (1) follows from Mott's law

$$\sigma = \exp[-(T_M/T)^{1/4}] \tag{2}$$

with $T_M = 16/[\xi^3 N(\varepsilon_F) k_B]$ and $N(\varepsilon_F) = W^{-1}V^{-1}k_BT/W$. The authors[2] suppose that the volume V is given by the length l of the metallic polyaniline strands and the interchain separation b, i.e., $V = b^2 l$. Since the nature of localization centers is *a priori* not known, we will use $V = d^3$, d being the average distance between localization centers. So we obtain Eq. (1) with

$$T_0 = 4W(d/\xi)^{3/2}/k_B. \tag{3}$$

This should be valid for $W \gg k_BT$. At higher temperatures the electrons will simply hop to the nearest localization center and an Arrhenius behavior is expected. The ratio of hopping distance to localization length is

$$\left(\frac{R}{\xi}\right)_0 = \frac{3}{8}\sqrt{\frac{T_0}{T}}$$

and displayed in Fig. 8 for $T = 100$ K, where $W > k_BT = 8.6$ meV holds (see Table I). We can also use Mott's law [Eq. (2)] to fit the temperature dependence of the conductivity, which results in a larger ratio R/ξ (see Fig. 8). Near f_c large values of R/ξ are measured corresponding to wide barriers or large hopping distances. At higher filling factors the hopping distance is nearly constant. Subramaniam *et al.*[3] have measured $T_0 = 938$ K for pure PAni (compressed Versicon powder) which gives $R/\xi \simeq 1.1$ at 100 K in agreement with the saturation value of the blends above $f \simeq 10\%$ (see Fig. 8, open circles). The further increase of conductivity with filling factor results from the addition of paths, but the barrier widths remain constant. This and the high absolute values of the conductivity suggest that the paths of PAni are completed and that there is probably no more insulating PETG incorporated. In addition, from

TABLE I. Parameters of blends above f_c according to Eq. (1) (100–300 K) and to $\sigma = \sigma_1 \exp(-W/k_BT)$ (200–300 K). d_T: see Eq. (4). For $f > 14\%$ the high-frequency value of the DF, ε_∞, could not be determined.

f [%]	σ_0 [Ω^{-1}m^{-1}]	T_0 [K]	σ_1 [Ω^{-1}m^{-1}]	W [meV]	ε_∞	d_T [nm]
9.02	8.9×10^{-3}	4848	1.1×10^{-5}	49.6		
10.03	3.6×10^{-3}	1154	1.1×10^{-3}	20.8	6.5	10.65
11.15	2.2×10^{-2}	931	8.8×10^{-3}	21.2	10.0	6.8
12.40	2.1×10^{-2}	697	9.0×10^{-3}	17.5	10.5	7.8
13.80	5.1×10^{-2}	674	2.3×10^{-2}	18.2	11.5	6.9
18.49	2.2	687	1.0	18.0		
27.99	37	509	18	14.7		

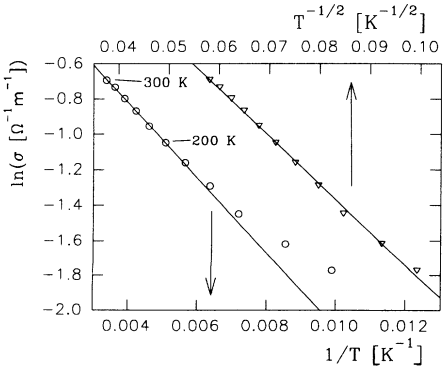

FIG. 7. Temperature dependence of the dc conductivity of a blend with $f = 18.5\%$. Circles: Arrhenius plot (lower x axis). Triangles: $\ln(\sigma_{dc})$ vs $1/\sqrt{T}$ (upper x axis).

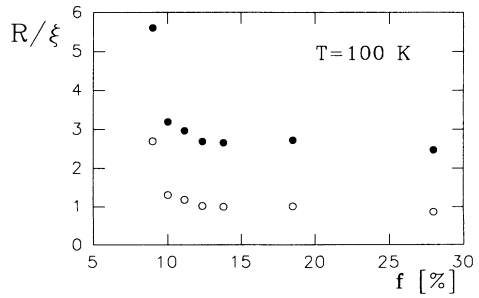

FIG. 8. Ratio of hopping distance to localization length vs filling factor at 100 K. Hollow circles: from Eq. (1), $R/\xi = (3/8)(T_0/T)^{0.5}$. Filled circles: from Mott's law [Eq. (2)], $R/\xi = (3/8)(T_M/T)^{0.25}$.

a small density stagnation around f_c and from pyrolysis experiments of carbon black filled polymers and of PAni blends it was concluded[25] that above f_c the adsorbed matrix layers break up at the contacts between neighbored regions of the dispersed component. Therefore, the conductivity is determined by paths of pure PAni, the transport mechanism of which can now be studied (the influence of a possibly remaining thin layer of PETG or additives will be discussed below). In addition, the temperature-independent ratio of localization length to mean distance between the centers can be calculated according to Eq. (3). Using the values of Table I we get $\xi \simeq d$ for $f > 10\%$ and $\xi < d$ for $f \leq 10\%$.

The size of the localization centers can be determined independent of a special hopping model or of an initial assumption on the localization length.[2] For both proposed transport mechanisms, hopping between metallic mesoscopic regions (like in a granular metal)[26] or intermolecular hopping between single metallic strands,[2] the activation energy W is given by the charging energy, i.e.,

$$W = \frac{1}{4\pi\varepsilon_0}\frac{e^2}{d_T}\left(\frac{1}{\varepsilon_\infty} - \frac{1}{\varepsilon_s}\right), \tag{4}$$

d_T being the 3D averaged diameter of the respective region to be charged. The static permittivity ε_s takes into account the energy lowering by polarization of the surrounding medium. Every localization center is surrounded by an effective medium, thus we can use in good approximation the experimental values of the measured permittivity of the blends. Since $\varepsilon_s \gg \varepsilon_\infty$ (Fig. 5) we can neglect the second term. ε_∞ is extrapolated from Cole-Cole diagrams (plot of the imaginary part of the DF vs the real part) and is nearly independent of temperature. The result for different filling factors above $f = 10\%$ (continuous flocculate structures of PAni) is given in Table I. For the 3D averaged diameter of the metallic regions between which hopping occurs follows

$$d_T \simeq 8 \text{ nm}.$$

The transport is therefore governed by 3D hopping between these mesoscopic metallic regions, the size of which is in agreement with the value obtained from the analysis of blends below f_c. Obviously, these regions correspond to the so-called primary particles which became visible in morphological studies of pure PAni.[5–7] Since the ratio of hopping distance to localization length R/ξ of blends above $f \simeq 10\%$ is constant and equals that of pure PAni (see above) we conclude that there is no significant change of the widths of insulating barriers even if some PETG molecules, additives or holes should remain in the conducting paths of the blends. Therefore, the barriers between the metallic crystalline regions in the conducting paths are mainly formed by amorphous PAni. The mean barrier width is $s = d - d_T = d_T(d/d_T - 1)$. About 30% of the PAni is crystalline, i.e., $0.3 \simeq (\pi/6)(d_T/d)^3$, thus we get $d_T/d \simeq 0.83$ and

$$s \simeq 1.6 \text{ nm}.$$

The size of a crystalline region with amorphous shell is $d = d_T + s \simeq 9.6$ nm, still in agreement with the size of the so-called primary particles (about 10 nm), and it equals the localization length (in the conducting paths holds $d \simeq \xi$, see above). Of course, even above f_c there will be some regions of PAni which are completly surrounded by the insulating matrix, but because of the enhanced barrier width their contribution to the effective conductivity can be neglected.

The dispersion of PAni in PETG above f_c results in smaller effective conductivity values compared to pure PAni and gives rise to a conduction current relaxation. But the transport mechanism (i.e., the thermal activation of the conductivity, barrier width, and hopping distance) remains unchanged because the conducting paths consist of pure PAni. Because of the lower conductivity (and because of the measurement technique) it is possible to determine the complex DF in a very large range of frequencies with its static and high-frequency values and thus to identify experimentally [according to Eq. (4), without any *a priori* assumptions on localization lengths] the nature and the size of the localization centers and barriers which dominate the charge transport (in pure fully protonated PAni only the high conductivity can be measured in the frequency range under discussion). We have confirmed the morphological picture which characterizes PAni as a collection of metallic islands separated by insulating barriers.[1] However, up to some GHz the conductivity is not determined by 1D interchain hopping in the amorphous parts,[1] by 3D hopping between single metallic molecular strands,[2] or by molecular scale disorder[27] which might become important at higher frequencies. Of course, a reduced microscopic disorder would decrease the height of the amorphous barriers.

We have shown that in the frequencv range from dc up to some GHz the conductivity of fully protonated polyaniline is governed by localization centers and barriers on a mesoscopic scale. The transport scenario is illustrated in Fig. 9. Two independent approaches (the enhancement of the quasistatic DF and the analysis of

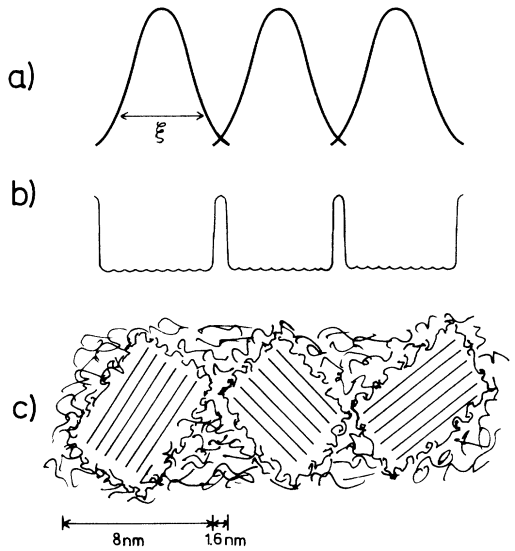

FIG. 9. Schematic view of (a) electronic wave functions (ξ: localization length), (b) potential, and (c) morphology of crystalline metallic regions and amorphous barriers.

the activation energy) yielded an 3D averaged diameter of the metallic regions in polyaniline of 8 nm. Three-dimensional hopping between these crystalline regions governs the transport mechanism, amorphous polyaniline serves as barrier. Therefore, PAni can be compared with a granular metal. The metallic mesoscopic regions with an amorphous shell ($d \simeq 10$ nm) correspond to the primary particles which were found in morphological studies previously.

We gratefully acknowledge financial support by the Deutsche Forschungsgemeinschaft, Bonn (Grant No. SFB 341/A3) and the Volkswagen–Stiftung (Project No. I/65 356).

[1] Z. H. Wang, E. M. Scherr, A. G. MacDiarmid, and A. J. Epstein, Phys. Rev. B **45**, 4190 (1992).
[2] Q. Li, L. Cruz, and P. Phillips, Phys. Rev. B **47**, 1840 (1993).
[3] C. K. Subramaniam, A. B. Kaiser, P. W. Gilberd, and B. Wessling, J. Polym. Sci. B **31**, 1425 (1993).
[4] C. O. Yoon, M. Reghu, D. Moses, and A. J. Heeger, Phys. Rev. B **48**, 14 080 (1993).
[5] B. Wessling, R. Hiesgen, and D. Meissner, Acta Polym. **44**, 132 (1993).
[6] B. Wessling, Synth. Met. **41-43**, 907 (1991).
[7] B. Wessling, Adv. Mater. **5**, 300 (1993).
[8] M. Reghu, Y. Cao, D. Moses, and A. J. Heeger, Phys. Rev. B **47**, 1758 (1993).
[9] R. Pelster, Ph.D. thesis, Köln, 1993; International Patent No. PCT/EP 92/02711 (pending).
[10] D. Stauffer, *Introduction to Percolation Theory* (Taylor & Francis, London, 1985), pp. 89–90.
[11] P. Hedvig, *Dielectric Spectroscopy of Polymers* (Adam Hilger LTD, Bristol, 1977), p. 398.
[12] J. van Turnhout, *Thermally Stimulated Discharge of Polymer Electrets* (Elsevier Scient., New York, 1975), pp. 222–223.
[13] N. G. McCrum, B. E. Read, and G. Williams, *Anelastic and Dielectric Effects in Polymeric Solids*, 2nd ed. (Dover, New York, 1967), pp. 501–520.
[14] R. Pelster (unpublished).
[15] L. K. H. van Beek, *Dielectric Behaviour of Heterogeneous Systems*, Progress in Dielectrics (Heywood, London, 1967), Vol. 7, pp. 69–114.
[16] G. Bánhegyi, Colloid Polym. Sci. **266**, 11 (1988).
[17] H. Looyenga, Physika **31**, 401 (1965).
[18] S. Stölzle, A. Enders, and G. Nimtz, J. Phys. I (France) 2, 401 (1992).
[19] S. Stölzle, A. Enders, and G. Nimtz, J. Phys. I (France) 2, 1765 (1992).
[20] M. Cini and P. Ascarelli, J. Phys. F **4**, 1998 (1974).
[21] E. M. Geniès, A. Boyle, M. Lapkowski, and C. Tsintavis, Synth. Met. **36**, 139 (1990).
[22] F. Zuo, M. Angelopoulos, A. G. MacDiarmid, and A. J. Epstein, Phys. Rev. B **39**, 3570 (1989).
[23] K. Yamamoto and H. Namikawa, Jpn. J. Appl. Phys. **28**, 2523 (1989).
[24] K. Yamamoto and H. Namikawa, Jpn. J. Appl. Phys. **31**, 3619 (1992).
[25] B. Wessling, Polym. Eng. Sci. **31**, 1200 (1991).
[26] C. J. Adkins, J. Phys. C **15**, 7143 (1982).
[27] K. Lee, A. J. Heeger, and Y. Cao, Phys. Rev. B **48**, 14 884 (1993).